Lasing properties of GaAs/(Al,Ga)As quantum-cascade lasers as a function of injector doping density

M. Giehler,[a] R. Hey, H. Kostial, S. Cronenberg, T. Ohtsuka, L. Schrottke, and H. T. Grahn
Paul-Drude-Institut für Festkörperelektronik, Hausvogteiplatz 5–7, 10117 Berlin, Germany

(Received 2 July 2002; accepted 6 December 2002)

The lasing properties of GaAs/$Al_{0.33}Ga_{0.67}$As quantum-cascade lasers are investigated as a function of injector doping concentration n_s between 2×10^{11} and 1×10^{12} cm^{-2} per period. Lasing is observed for $n_s \geqslant 3.5\times10^{11}$ cm^{-2}, with optimal lasing properties (minimum of the threshold current and maximum of the modified characteristic temperature) for $n_{\rm opt} \approx 6\times10^{11}$ cm^{-2}. With increasing n_s up to $n_{\rm opt}$, the lasing energy of 115 meV exhibits first a blueshift to 135 meV, followed by a redshift to 120 meV for higher doping levels. This shift of the lasing energy as a function of n_s is discussed in terms of changes in the field distribution, occupation of additional levels above the upper laser level, and electron–electron interactions.
[DOI: 10.1063/1.1541099]

In the last eight years, the development of quantum-cascade lasers (QCLs) as light emitters for the midinfrared region has achieved a number of major breakthroughs.[1] In 1994, Faist *et al.*[2] demonstrated pulsed laser emission for an (In,Ga)As/(In,Al)As QCL grown lattice matched on InP at cryogenic temperatures. Four years later, Sirtori *et al.*[3] achieved pulsed operation at low temperatures for a GaAs/(Al,Ga)As QCL grown on GaAs. Very recently, cw operation at room temperature was reported for an (In,Ga)As/(In,Al)As QCL,[4] a broadband QCL based on (In,Ga)As/(In,Al)As covering a spectral range from 5 to 8 μm[5] and the first QCL operating at an energy below the optical phonon energy of the constituent materials GaAs/(Al,Ga)As[6] were demonstrated. For a comprehensive review of earlier developments of QCLs, see Ref. 7.

At first, the research focused on the quantum design of the optically active region in order to maximize the gain of the lasing transition. Later, the injector region was designed in order to optimize the electron transfer from the injector reservoir into the upper lasing level as well as the electron transfer from the active region into the next injector stage.[7] However, there has been no report of a detailed study on the influence of the doping density on the lasing properties.

In this letter, we present a study of the lasing properties of GaAs/(Al,Ga)As QCLs as a function of the doping density n_s. With increasing n_s, the lasing energy first exhibits a significant blueshift up to intermediate doping levels, followed by a redshift at even higher doping levels. At intermediate doping levels, the threshold current density (modified characteristic temperature) exhibits a minimum (maximum).

We have used the well established GaAs/$Al_{0.33}Ga_{0.67}$As QCL with plasmon-assisted waveguides. The design of this QCL was introduced by Sirtori *et al.*[3,8] The number of periods was set to 30 in each QCL. The samples were grown by molecular-beam epitaxy at a substrate temperature of 600 °C. The Si doping concentration n_s at the four center layers of the injector region was varied between 2.3×10^{11} and 1.0×10^{12} cm^{-2} per period. All QCL structures were characterized by double-crystal x-ray diffraction measurements to demonstrate that the actual layer thicknesses as well as the Al content agree within 2% with the nominal values. The sheet carrier concentration was determined by capacitance–voltage measurements on step-etched pieces showing good agreement with the nominal values. After growth, laser stripes with typical dimensions of 19×2400 μm^2 were prepared by plasma etching. The side walls of the lasers were defined by 7 μm deep and 2.5 μm broad trenches, which were refilled by a photoresist.

The laser emission was studied using pulse-mode operation with a width of 100 ns and a repetition rate of 5 kHz. The infrared spectra were recorded using a Fourier-transform spectrometer with a spectral resolution of 0.015 meV. The QCLs were mounted on a cold finger in a He-flow cryostat without exchange gas and heat management. All spectra were measured at 8 K and for a current density j just above the threshold current density $j_{\rm th}$, i.e., $j \approx 1.1\, j_{\rm th}$.

Figure 1 shows the lasing spectra of QCLs for n_s between 3.5×10^{11} and 1.0×10^{12} cm^{-2} increasing from top to bottom as indicated. The top panel for $n_s = 3.5\times10^{11}$ cm^{-2} shows spectra for three different pieces of the same wafer, indicating that the lasing energy varies by no more than about 1 meV. For $n_s = 2.3\times10^{11}$ cm^{-2}, lasing was not observed. While the total width of the energy window is kept constant at 2 meV, the emission energy E_0 shifts with increasing n_s by about 20 meV to higher energies, until the doping density exceeds 5.3×10^{11} cm^{-2}. It then decreases by about 15 meV for values of n_s up to 1.0×10^{12} cm^{-2}. Note that this change of the lasing energy due to the doping variation is more than one order of magnitude larger than variations of E_0 across a wafer. Furthermore, since we verified the structural parameters of the QCLs by x-ray diffraction, we can also exclude that the variation of E_0 is caused by fluctuations of the layer thickness or Al content.

Figure 2 shows the temperature dependence of the threshold current density $j_{\rm th}(T)$ in a semilogarithmic repre-

[a]Author to whom correspondence should be addressed; electronic mail: giehler@pdi-berlin.de

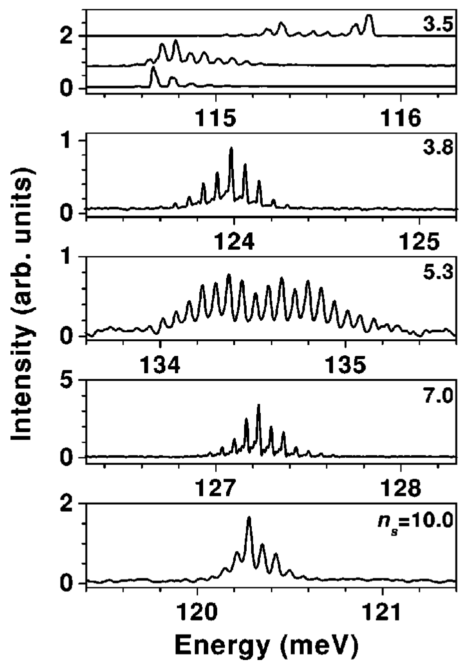

FIG. 1. Emission spectra of $GaAs/Al_{0.33}Ga_{0.67}As$ QCLs for various values of n_s (in units of $10^{11}\ cm^{-2}$) as indicated. The spectra for $n_s = 3.5 \times 10^{11}\ cm^{-2}$ correspond to three different pieces from the same wafer. The intensity scales of the different panels are directly comparable.

sentation for differently doped QCLs. The QCL with $n_s = 5.3 \times 10^{11}\ cm^{-2}$ exhibits the lowest $j_{th}(T)$ values with a low-temperature value of $5.1\ kA\,cm^{-2}$ as well as a linear high-temperature region in the semilogarithmic representation. It also exhibits the highest maximum operating temperature T_{max} of 180 K of all QCLs for a driving current of 10 A. A fit of this high-temperature region with the expression $j_{th}(T) \propto \exp(T/T_0)$ results in a characteristic temperature

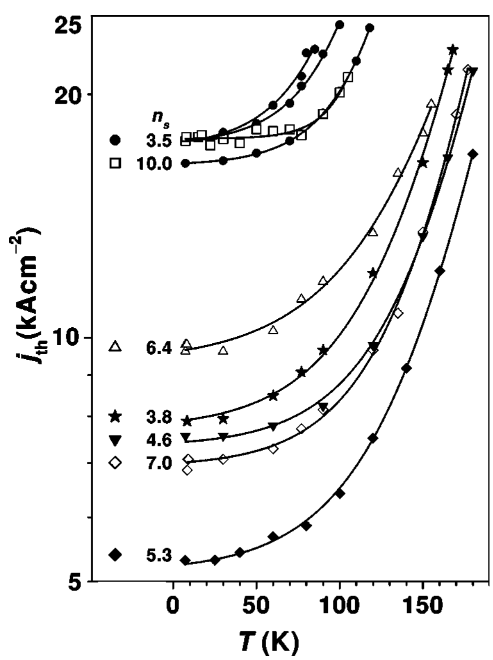

FIG. 2. Temperature dependence of the threshold current density for QCLs with different doping levels (in units of $10^{11}\ cm^{-2}$) as indicated. The curves for $n_s = 3.5 \times 10^{11}\ cm^{-2}$ correspond to three different pieces from the same wafer. The symbols denote experimental data, the solid lines correspond to fits of the data with Eq. (1).

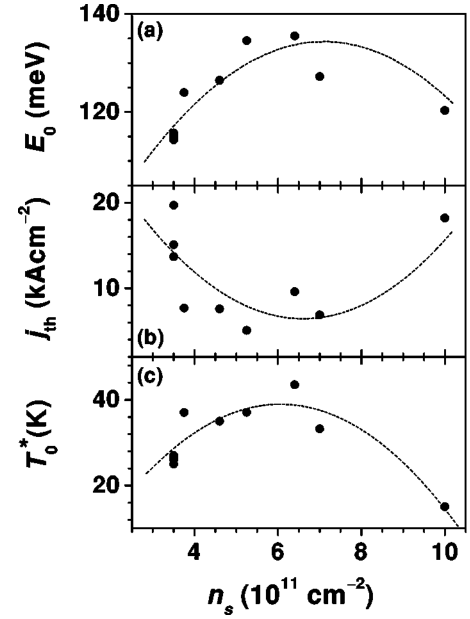

FIG. 3. (a) Lasing energy E_0, (b) threshold current density j_{th}, and (c) modified characteristic temperature $T_0^\star$ vs doping density n_s for the different QCLs.

T_0 of 60 K. The QCLs with smaller and larger n_s exhibit larger $j_{th}(T)$ and lower T_{max} values. In particular, the QCLs with the smallest and largest values of n_s do not follow the expression for $j_{th}(T)$ given above, since the low-temperature value of j_{th} becomes too large. However, by using the expression

$$j_{th}(T) = j_0 + A \exp(T/T_0^\star), \tag{1}$$

where j_0, A, and $T_0^\star$ (modified characteristic temperature) denote fitting parameters, excellent fits for all QCLs over the whole operating temperature range can be obtained as indicated by the solid lines in Fig. 2. From these fits, we obtain $j_0 \approx j_{th}(T = 8\ K)$ for all QCLs.

In Figs. 3(a), 3(b), and 3(c), E_0, $j_{th}(T = 8\ K)$, and $T_0^\star$, respectively, are plotted as a function of n_s. The value of E_0 was determined by taking the energy, for which the integral over part of the laser modes up to E_0 becomes one half of the integral over all laser modes. The dashed lines indicate fits to the data points using a quadratic polynomial. While E_0 and $T_0^\star$ exhibit a maximum, j_{th} shows a minimum for $n_s \approx 6 \times 10^{11}\ cm^{-2}$. Therefore, this particular doping level will be called the optimal doping density n_{opt}. The QCL with $n_s = 5.3 \times 10^{11}\ cm^{-2} \approx n_{opt}$ exhibits values for E_0 and j_{th}, which are in good agreement with those published by Sirtori *et al.*[8] for $GaAs/Al_{0.33}Ga_{0.67}As$ QCLs. The maximum peak output power of this QCL measured with a power meter at a driving current density of $j \approx 3 j_{th}$ at 8 K was determined to be 450 mW, which is also comparable with the corresponding value given in Ref. 8.

Figure 3 clearly shows that there is an optimal doping level n_{opt} for lasing. The doping of the injector region has two functions, first the supply of electrons and second to prevent the buildup of space charge in the QCL. For resonant injection into the upper laser level, the current density in the QCL is given by $j = e n_s/(2\tau_3)$,[9] where τ_3 denotes the lifetime of the electrons in the upper laser level and e the electron charge. Although population inversion can be achieved

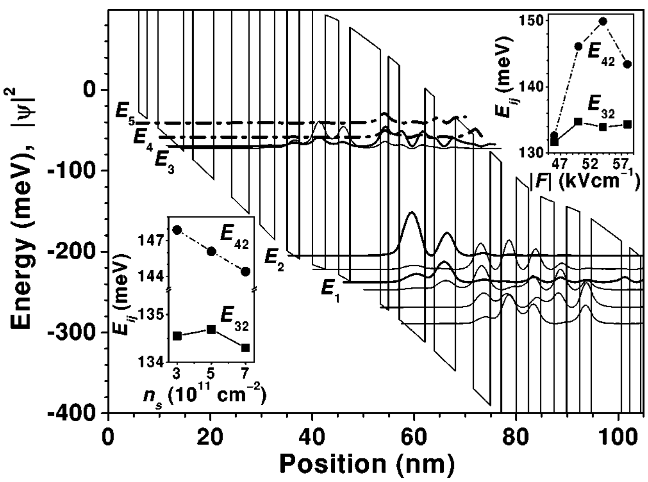

FIG. 4. Calculated conduction band diagram of the GaAs/$Al_{0.33}Ga_{0.67}As$ QCL with $n_s = 5\times10^{11}$ cm^{-2} for $F = 50$ kV cm^{-1}. The left (right) inset displays the energy shift E_{ij} for $F = 50$ kV cm^{-1} ($n_s = 5\times10^{11}$ cm^{-2}) as a function of n_s (F).

in principle for any value of n_s, the carrier density and the resulting current have to be sufficiently large so that the gain becomes larger than the losses. Therefore, the laser does not work below a certain value of n_s. At the same time, n_s should be as low as possible, because an increasing value of n_s increases the scattering rate of electrons from the injector back into the active region[9] and the optical losses due to free-carrier absorption. Both effects will reduce the gain.[7] Consequently, we expect a certain range of values of n_s, for which the laser will operate, and furthermore an optimal density, for which j_{th} becomes minimal and $T_0^\star$ maximal.

While the existence of an optimal value for j_{th} and $T_0^\star$ can be qualitatively explained as discussed above, the variation of E_0 as a function of n_s may be caused by several effects. In order to determine the influence of n_s on the field distribution and therewith on the lasing transition energy, we have carried out self-consistent band structure calculations based on the Schrödinger and Poisson equations for n_s between 3×10^{11} and 7×10^{11} cm^{-2} and for external electric field strength F between 46 and 58 kV cm^{-1} neglecting many-particle effects. Figure 4 shows the conduction band diagram calculated for a QCL with $n_s = 5\times10^{11}$ cm^{-2} at $F = 50$ kV cm^{-1}. The depopulation level for the lower laser level, the lower and the upper laser levels with energies E_1, E_2, and E_3, respectively, are indicated as thick solid lines. For the energy separation between the laser levels denoted by $E_{32} = E_3 - E_2$, we obtain about 134 meV, which corresponds to the measured value of E_0. The left (right) inset of Fig. 4 shows that for $F = 50$ kV cm^{-1} ($n_s = 5\times10^{11}$ cm^{-2}) the transition energy E_{32} varies by less than 1 meV (3 meV) as a function of n_s (F). Therefore, the calculated variation ΔE_{32} is much smaller than the largest observed shift of E_0 of 20 meV. However, additional levels denoted by E_4 and E_5, which are located 10–25 meV above the upper laser level E_3, are also included in Fig. 4 as thick dash-dotted lines. The left (right) inset of Fig. 4 shows the shift of the transition energy $E_{42} = E_4 - E_2$ as a function of n_s (F) for $F = 50$ kV cm^{-1} ($n_s = 5\times10^{11}$ cm^{-2}). With increasing n_s, the energy of E_4 decreases with respect to E_3 so that E_4 becomes more and more occupied. This may contribute to the observed blueshift of E_0 from the low to the optimal doping level. Further calculations with an improved model are necessary to unambiguously identify the origin of the blue- and redshift with increasing n_s.

In the high-doping regime, E_0 can also depend on n_s through the nonparabolicity of the band structure as well as electron–electron interactions, such as the depolarization shift and the intersubband exchange interaction. The dependence of the intersubband transition energy on n_s for this material system has been studied by intersubband absorption and electronic Raman scattering experiments.[10–14] However, all experimental data in the literature were obtained under thermal equilibrium condition, which is very different from the situation in an operating QCL. In order to calculate the shift of E_0 quantitatively, a more detailed knowledge of the intersubband emission process for a highly occupied upper subband and weakly occupied lower subband is necessary. Furthermore, the much more complex structure of the QCL with respect to the MQW structures discussed in the literature has also to be taken into account.

In summary, the lasing properties of GaAs/$Al_{0.33}Ga_{0.67}As$ QCLs have been studied as a function of injector doping density n_s. For j_{th} and $T_0^\star$, there exists an optimal value of $n_{opt} \approx 6\times10^{11}$ cm^{-2}. In order to unambiguously determine the origin of the observed variation of the lasing energy with n_s, a more detailed modelling of the QCLs as a function of n_s is necessary, which should also include many particle effects.

The authors would like to thank D. Heitmann and M. Ramsteiner for helpful discussions. This work was supported in part by the Deutsche Forschungsgemeinschaft within the framework of the Forschergruppe 394.

[1] F. Capasso, C. Gmachl, D. L. Sivco, and A. Y. Cho, Phys. Today **55**, No. 5, 34 (2002).
[2] J. Faist, F. Capasso, D. L. Sivco, C. Sirtori, A. L. Hutchinson, and A. Y. Cho, Science **264**, 553 (1994).
[3] C. Sirtori, P. Kruck, S. Barbieri, P. Collot, J. Nagle, M. Beck, J. Faist, and U. Oesterle, Appl. Phys. Lett. **73**, 3486 (1998).
[4] M. Beck, D. Hofstetter, T. Aellen, J. Faist, U. Oesterle, M. Ilegems, E. Gini, and H. Melchior, Science **295**, 301 (2002).
[5] C. Gmachl, D. L. Sivco, R. Colombelli, F. Capasso, and A. Y. Cho, Nature (London) **415**, 883 (2002).
[6] R. Köhler, A. Tredicucci, F. Beltram, H. E. Beere, E. H. Linfield, A. G. Davies, D. A. Ritchie, R. C. Iotti, and F. Rossi, Nature (London) **417**, 156 (2002).
[7] C. Gmachl, F. Capasso, D. L. Sivco, and A. Y. Cho, Rep. Prog. Phys. **64**, 1533 (2001).
[8] C. Sirtori, P. Kruck, S. Barbieri, H. Page, J. Nagle, M. Beck, J. Faist, and U. Oesterle, Appl. Phys. Lett. **75**, 3911 (1999).
[9] C. Sirtori, F. Capasso, J. Faist, A. L. Hutchinson, D. L. Sivco, and A. Y. Cho, IEEE J. Quantum Electron. **34**, 1722 (1998).
[10] M. Załużny, Phys. Rev. B **49**, 2923 (1994).
[11] M. Ramsteiner, J. D. Ralston, P. Koidl, B. Dischler, H. Biebl, J. Wagner, and H. Ennen, J. Appl. Phys. **67**, 3900 (1990).
[12] U. Ekenberg, Phys. Rev. B **40**, 7714 (1989).
[13] P. von Allmen, M. Berz, G. Petrocelli, F.-K. Reinhard, and G. Harbeke, Semicond. Sci. Technol. **3**, 1211 (1988).
[14] W. L. Bloss, Solid State Commun. **46**, 143 (1983).